Modeling of Heterogeneous Systems in a Plasma Jet Reactor

A theoretical model of the behavior of a plasma jet reactor (5 000 K to 12 000 K) considering a three-dimensional, nonisothermal, turbulent, compressible, swirling, confined flow is developed. Single particle trajectories are predicted by solving the equations of motion for the axial, radial, and tangential directions. Calculations are carried out for both argon and nitrogen gases. The model is then extended to a multiparticle system on the basis of a feed particle size distribution, concentration distribution, and loading ratio.

The calculations are applied to a study of the decomposition of molybdenum disulfide particles into molybdenum metal and elemental sulfur. Results are presented in terms of the effects on the particle history (trajectory, temperature, and conversion) of the following variables: particle size, nozzle exit temperature and velocity, injection velocity, location and angle of injection, swirl velocity, and ambient temperature conditions.

D. BHATTACHARYYA and W. H. GAUVIN

Department of Chemical Engineering*
McGill University, Montreal, Canada

SCOPE

The application of high temperature plasmas in chemical and metallurgical operations is of increasing interest in a variety of commercial processes, for example, in chemical synthesis, spectroscopy, pyrometallurgy, spheroidization, spray coating, crystal growth, ion implementation, and many others. The temperature in a plasma column varies in the range of 5 000 K to 50 000 K, depending upon the operating conditions and the arc atmosphere. In spite of the high temperatures generated, plasma devices are not necessarily efficient sources of heat in gas-solid reactions. This is due to the fact that the particulate reagents often bypass the hottest zone rather than penetrate it, thus resulting in a poor heat transfer to the particles (Freeman, 1969). It is obvious that a plasma jet is three-dimensional in nature. Expansion of a hot jet gives rise to radial fluid motion and hence to radial particle motion. The swirling motion of the plasma, which is generally present for consideration of stability, may also have a substantial effect on particle migration, especially in the radial direction. Due to the extremely short contact period (about 4 to 5ms) of the particles in high enthalpy plasma streams, the feasibility of a plasma process largely depends upon an accurate knowledge of the fluid dynamics properties of the system. The latter enables the proper control of particle trajectories and consequently of their thermal histories and degree of conversion.

An analysis of particle residence time criteria in a nonequilibrium plasma spray gun is given in a recent paper by Maxwell (1974).

Domingos and Roriz (1974) recently presented the most realistic model to date to calculate the trajectories of evaporating droplets in a three-dimensional flow with swirl. However, the effects of Coriolis and centrifugal forces were not taken into account. A few attempts have been made in the past to simulate the behavior of solid particles in highly nonisothermal and compressible plasma flames. Sheer et al. (1973) studied the arc vaporization of refractory powders. Two-dimensional (neglecting swirl) trajectories were calculated on the basis of a force balance. The most comprehensive model in predicting the particle trajectories and temperature history in a plasma flame was presented by Boulos and Gauvin (1974). However, their model was one dimensional as far as the gas flow is concerned, and the stabilizing swirl flow was neglected.

The objective of this work was to investigate the fluid dynamics and heat transfer characteristics of a plasma jet reactor for particle-gas contacting over a wider range of operating conditions and flow complexities than has heretofore been studied. A theoretical model has accordingly been developed to simulate a plasma jet reactor, considering a three-dimensional, nonisothermal, turbulent, compressible swirling confined flow. Known velocity and thermal profiles are introduced as input parameters. The formulation is highly flexible and applicable to the tail portion of both direct current and radio frequency plasmas as well as to those with multiple jets and transferred arcs, irrespective of the way in which the solid particles are introduced. The decomposition of molybdenite (MoS_2) particles into molybdenum metal and elemental sulfur was used as a specific application of the model.

CONCLUSIONS AND SIGNIFICANCE

A detailed analysis is carried out to predict the particle trajectories and temperature history in three-dimensional motion for a particle injected in a plasma tail-flame and undergoing thermal decomposition. The governing equations of force balance including drag, gravity, buoyancy, Coriolis, centrifugal and lift forces are developed. The added contributions of mass and history terms in the Basset-Boussinesq-Oseen equation and that of the thermophoretic effect are also considered. Particle size distribution, concentration distribution, injection velocity and location, swirl parameter and the angle of injection of the feed are the important parameters. In general, an increase in the conversion is observed with an increase in the ratio of the ambient to the gas temperature at the virtual origin. High solid loadings quench the gas and lower the reaction rate. However, low solid loading ($L \leq 0.25$) has insignificant effects on the overall conversion provided

* Present address: Direction Sciences de Base, Institut de Recherche de l'Hydro-Québec, Varennes, Québec, Canada.

sufficient residence time is available.

The principal significance of the work is that it provides a far better insight into the process than would otherwise be possible. The simulation has clearly indicated the relative importance of the major parameters, such as particle injection and degree of swirl on the extent of the conversion. Also, as a result of the comparative studies of argon and nitrogen plasmas, an economic survey is made possible in the light of the present data on the conversion and power requirements. This in turn provides confidence in the process of scaling-up from the pilot-plant stage to the full industrial production unit and may eliminate some of the intermediate stages at, possibly, a considerable saving in time and capital cost.

JET EQUATIONS

A plasma tail-flame has all the properties of a nonisothermal, compressible jet. The classical theory of jet mixing (Townsend, 1956) considers three main regions, namely the potential core, the transition region, and the developed zone. A schematic diagram of the system is shown in Figure 1. The axial velocities at different regimes under isothermal conditions are

Core region:

$$r \leq r_1 \quad V_{fz} = V_0 \tag{1}$$

$$r > r_1 \quad V_{fz} = V_0 \exp\left[-\ln 2(r^2 - r_1^2)/(r_5^2 - r_1^2)\right] \tag{2}$$

Developed region:

$$r > 0 \quad V_{fz} = V_c \exp\left[-\ln 2(r/r_5)^2\right] \tag{3}$$

For a highly nonisothermal and compressible jet, Gal (1970) proposed a correlation for the center line velocity

$$V_c = V_0\, 6.5/(z/D_0^1) \tag{4}$$

where

$$D_0^1 = D_0(\rho_0/\rho_\infty)^{1/2} \tag{5}$$

The above correlations are applicable to a nonswirling, free plasma jet. However, a number of theoretical studies have been carried out for laminar swirling jets by many authors (Görtler, 1954; Loitsyanskii, 1953). Chigier and Beér (1964) and Chigier and Chervinsky (1966, 1967) studied turbulent swirling jets.

Chigier and Chervinsky (1967) applied the principle of similarity to the integral Reynolds equations of motion and obtained theoretical expressions for axial and tangential velocities as follows:

$$V_c/V_{cn} = K_1(D_0/z)f_1^{1/2} \tag{6}$$

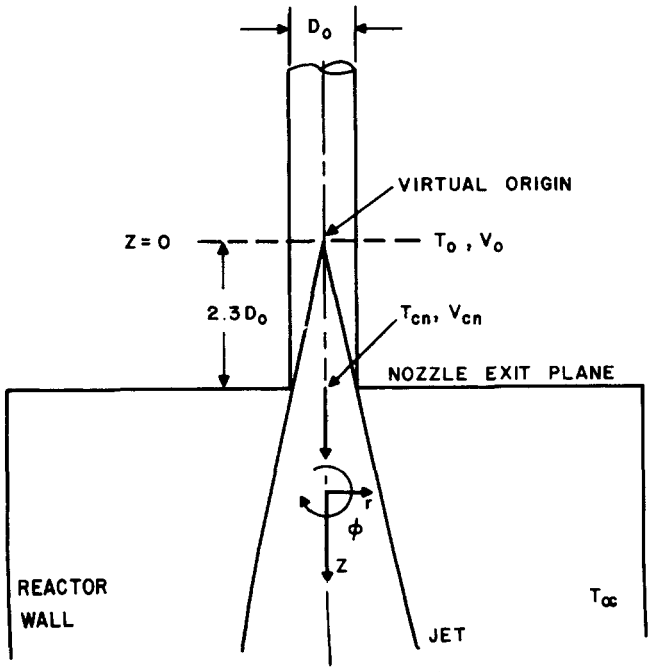

Fig. 1. Schematic diagram of system.

$$V_m/V_{\phi m} = K_2(D_0/z)^2 f_2^{-1/2} \tag{7}$$

Empirical values of f_1 and f_2 are presented as functions of $G = V_{\phi m}/V_{cn}$. The experimental results showed that with the increase in swirl the jet core length decreased substantially and finally vanished. They defined a new dimensionless swirl parameter $S = G_\phi/(G_z R_0)$ and it was approximated as

$$0 \leq G \leq 0.4 \quad S = G/2/[1 - (G/2)^2] \tag{8}$$

$$0.4 < G \quad S = G/2/[(1 - G/2)] \tag{9}$$

The measured axial velocity followed the Gaussian error equation

$$V_{fz}/V_c = \exp\left[-K_3(r/z)^2\right] \tag{10}$$

The experimental values of the constants K_1, K_2, and K_3 are

$$K_1 = 6.8/(1 + 6.8S^2) \tag{11}$$

$$K_2 = 5.3 \tag{12}$$

$$K_3 = 92/(1 + 6S) \tag{13}$$

The similar swirl velocity profile is described by a third-order polynomial:

$$V_{f\phi}/V_m = A\xi + B\xi^2 + C\xi^3 \tag{14}$$

where

$$\xi = r/z$$

Pratte and Keffer (1969, 1972) measured the effect of swirl parameter on axial, radial, and tangential velocities. Kerr and Fraser (1965) and Kerr (1965) studied the effect of swirl on flame performance. Kerr (1965) made a simplified cold modeling of swirling flames based on the conservation of axial momentum as proposed by Thring and Newby (1953). Chedaille et al. (1966) experimentally studied the effects of swirl on coaxial hot jets under free and confined conditions.

It is known that the aerodynamic flow patterns of a confined jet can differ profoundly from that of a free jet. Becker et al. (1963) showed a Gaussian error function for the axial velocity distribution

$$V_{fz}/V_c = \exp\left[-\ln 2(r/r_5)^a\right] \tag{15}$$

where the average value of $a = 1.82$ represented all the data quite accurately.

FORMULATION

The gas velocity and temperature profiles are required as input parameters and are obtained from literature with certain assumptions and modifications. Since it is known that both confined and free-jet equations for nonswirling conditions are Gaussian, and that, moreover, swirling and nonswirling free-jet equations are similar in nature, it is assumed that the equation for axial swirling flow, as given by Chigier and Chervinsky (1967) could be extended to confined flows with the change in exponent from 2 to $a = 1.82$ as follows:

$$V_{fz}/V_c = \exp\left[-K_3(r/z)^a\right] \tag{16}$$

where for present conditions:

$$V_c = V_{cn} K_1 (D_0{}^1/z) f_1{}^{1/2} \quad (17)$$

The assumed tangential velocity is given by

$$V_m = V_{\phi m} K_2 (D_0{}^1/z)^2 f_2{}^{-1/2} \quad (18)$$

The fluid radial velocity is calculated numerically from the continuity equation

$$\partial(\rho_f V_{fz})/\partial z + (1/r)\, \partial(\rho_f r V_{fr})/\partial r + (1/r)\, \partial(\rho_f V_{f\phi})/\partial\phi = 0 \quad (19)$$

It is assumed that the flow is symmetric, that is,

$$\partial(\rho_f V_{f\phi})/\partial\phi = 0$$

Extending O'Connor et al.'s (1966) correlation for a compressible nonisothermal plasma jet, the temperature profile is

$$(T - T_\infty)/(T_c - T_\infty) = (V_{fz}/V_c)^b \quad (20)$$

where $b = Pr_t{}^{a/2}$ and for $Pr_t = 0.64$, $b = 0.666$. The center line temperature T_c is calculated from

$$(T_c - T_\infty)/(T_0 - T_\infty) = V_c/V_0 \quad (21)$$

The values of the functions f_1 and f_2 in Equations (17) and (18), respectively, and the constants A, B and C in Equation (14) are taken from the experimental data of Chigier and Chervinsky (1967) for different swirl parameters.

The gas velocities are assumed to be unaffected by particle loading (in the multiparticle case up to $L \leq 0.25$). The temperature profile is corrected on the basis of total heat loss due to sensible heat, reaction, and radiation.

PARTICLE TRAJECTORY

Axial, radial, and tangential velocities of the gas are taken into account to predict the path of a single particle in flight. The trajectories are calculated by solving the Basset-Boussinesq-Oseen equation:

$$-F = C_D(\pi D_p{}^2 \rho_f/8)\, U_r|U_r| + C_A(\pi D_p{}^3 \rho_f/6)\, dU_r/d\theta + C_H(D_p{}^2/4) \times \sqrt{\pi\rho_f\mu_f} \int_{\theta_0}^{\theta} (dU_r/d\theta)\, d\theta^1/\sqrt{\theta - \theta^1} + \text{body force} \quad (22)$$

It was reported by Boulos and Gauvin (1974) that the Basset history and added mass terms may be neglected provided the particle equivalent sphere diameter is less than 30 μm. Sheer et al. (1973) showed that the thermophoretic force for silica particles of $D_p > 20$ μm is insignificant.

In a three-dimensional flow the forces acting are: buoyancy force in all directions, plus (1) drag and gravity in the axial direction; (2) drag, centrifugal, and lift in the radial direction; and (3) drag and Coriolis forces in the angular direction. Therefore, a force balance gives

$$dV_{pz}/d\theta = (\rho_f/\rho_p)\, dV_{fz}/d\theta - 3C_D\rho_f(V_{pz} - V_{fz}) \times |V_{pz} - V_{fz}|/(4D_p\rho_p) + g(1 - \rho_f/\rho_p) \quad (23)$$

$$dV_{pr}/d\theta = (\rho_f/\rho_p) dV_{fr}/d\theta - 3C_D\rho_f(V_{pr} - V_{fr}) \times |V_{pr} - V_{fr}|/(4D_p\rho_p) + [1 - (\rho_f/\rho_p)V_{fr}{}^2/V_{p\phi}{}^2]V_{p\phi}{}^2/R_p + \sqrt{\nu_f K}\,(V_{p\phi} - V_{f\phi})81\rho_f/(2D_p\rho_p) \quad (24)$$

$$dV_{p\phi}/d\theta = (\rho_f/\rho_p) dV_{f\phi}/d\theta - 3C_D\rho_f(V_{p\phi} - V_{f\phi}) \times |V_{p\phi} - V_{f\phi}|/(4D_p\rho_p) - [1 - (\rho_f/\rho_p)V_{f\phi}{}^2/(V_{p\phi}V_{pr})]V_{p\phi}V_{pr}/R_p \quad (25)$$

where K is the curl of the fluid velocity and given by (Saffman, 1965; Lawler and Lu, 1970):

$$K = 1.4\, V_{fz}(r/r_5{}^2) \quad (26)$$

The above formulation is similar to those used by Gauvin et al. (1975) in their model for predicting the drop trajectories in a spray dryer (with no radial temperature variation).

The calculations are carried out for MoS_2 powder (30 to 75 μm flakes) with an aspect ratio e of 0.025. The particle drag coefficients are estimated for thin disks moving with their cross section of largest area perpendicular to the direction of motion.

Range	C_D	Reference
$Re < 0.1$	$24S^1/Re$	Happel and Brenner (1965) (27)
$0.1 \leq Re < 1.0$	$(1 + 3S^1Re/16)\ 24S^1/Re$	Aoi (1955) (28)
$1.0 \leq Re < 20$	$(1 + 0.136Re^{0.803})\ 20.4/Re$	Masliyah and Epstein (1970) (29)
$20 \leq Re < 100$	$(1 + 0.138Re^{0.793})\ 20.4/Re$	Masliyah and Epstein (1970) (30)

For thin disks, shape factor, $S^1 = 8/(3\pi)$ and the equivalent particle diameter is

$$D_p{}^1 = D_p(0.5 + e) \quad (31)$$

Once the particle reaches its melting point, it is assumed to be spherical and the drag coefficient values are

Range	C_D	Reference
$Re < 0.2$	$24/Re$	Stokes' solution (32)
$0.2 \leq Re < 2.0$	$(1 + 3Re/16)\ 24/Re$	Oseen's solution (33)
$2.0 \leq Re < 21$	$(1 + 0.11Re^{0.810})\ 24/Re$	Beard and Pruppacher (1969) (34)
$21 \leq Re < 200$	$(1 + 0.189Re^{0.632})\ 24/Re$	Beard and Pruppacher (1969) (35)

All C_D values are first calculated at the average film temperature and modified for the steep temperature gradient as suggested by Lewis and Gauvin (1973):

$$C_D = (C_D)_{av}\, (\nu_{av}/\nu_f)^{0.15} \quad (36)$$

PARTICLE CONVERSION

It has been shown by Munz (1974) that the reaction

$$MoS_2 \rightarrow Mo + S_2 \quad (37)$$

is heat transfer controlled and MoS_2 starts reacting appreciably in the solid state from 1 773 K.

In flight, the moving particles go through the following phases:

(1) $T_p < 1\,773$ K — Solid state (flake): no reaction, only heating

(2) $1\,773\ \text{K} \leq T_p < 1\,923$ K — Solid state (flake): (i) heating of $MoS_{2(s)}$ (ii) conversion of $MoS_{2(s)} \rightarrow Mo_{(s)} + S_{2(v)}$ (iii) heating of converted $Mo_{(s)}$

(3) $T_p = 1\,923$ K — Melting: (i) heat for melting of $MoS_{2(s)}$ (ii) conversion of $MoS_{2(s)} \rightarrow$

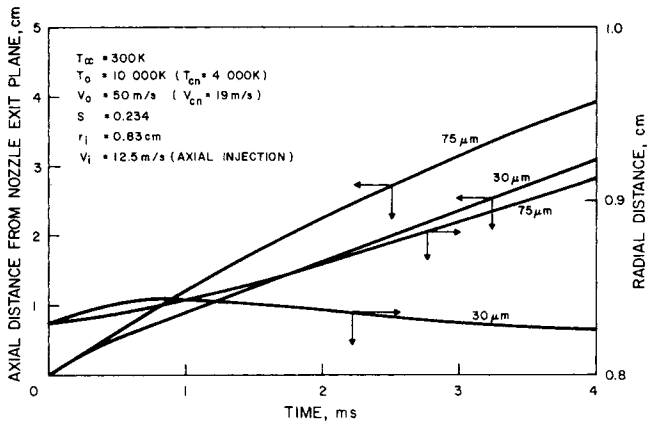

Fig. 2. Axial and radial displacements of particle in flight.

		$Mo_{(s)} + S_{2(v)}$ (converted Mo stays at 1 923 K)
(4)	1 923 K $\leq T_p$ < 2 892 K	Solid-liquid state: (i) conversion of $MoS_{2(l)} \rightarrow Mo_{(s)} + S_{2(v)}$ (ii) heating of $MoS_{2(l)}$ (iii) heating of $Mo_{(s)}$ (continues till complete conversion takes place)
(5)	T_p = 2 892 K	Melting: $Mo_{(s)} \rightarrow Mo_{(l)}$
(6)	2 892 K < T_p < 4 919 K	Heating of liquid Mo
(7)	T_p = 4 919 K	Vaporizing: $Mo_{(l)} \rightarrow Mo_{(v)}$ (Mo vapour causes loss in Mo recovery).

The data for these mentioned physical and chemical changes are taken from Munz (1974) and JANAF (1967).

The particle temperature in flight is calculated from a heat balance. The Ranz and Marshall (1952) correlation

$$Nu = 2 + 0.6\, Re^{1/2} Pr^{1/3} \qquad (38)$$

is used for pure heat transfer. Whereas in the presence of reaction, the heat transfer equation of Ross and Hoffman (1966)

$$Nu = (2 + 0.369\, Re^{0.58} Pr^{1/3})\,(1 + B^1)^{-0.6} \qquad (39)$$

is used, which includes the effect of mass transfer (due to sulfur generation).

The Nusselt number values are also corrected (Lewis and Gauvin, 1973):

$$Nu = (Nu)_{av}\,(\nu_{av}/\nu_f)^{0.15} \qquad (40)$$

An emissivity value of 0.55 is used to estimate the radiative heat losses assuming that the gas is optically thin.

The model is then extended to a multiparticle system (for its commercial application) on the basis of feed particle size, distribution, and particle loading.

RESULTS AND DISCUSSION

The ranges of the different parameters studied were

Particle size:	30-75 μm (flake)
Virtual origin velocity:	20-100 m/s
Nozzle exit velocity:	7.6-38 m/s
Injection velocity:	5-25 m/s
Swirl:	0.066-0.640
Virtual origin temp.:	5 000-12 000 K
Nozzle exit temp.:	2 000-4 800 K
Ambient temp.:	300-1 000 K
Angle of injection:	0°-135°
Injection location:	Center to the boundary of the jet
Particle loading:	0-0.25 g/g of gas

In all cases, the particles have been considered as being injected at the nozzle exit plane which lies at a distance of 2.3 D_0 from the virtual origin of the jet. Therefore, the conditions at both virtual origin and nozzle exit plane are given.

A typical single particle trajectory is shown in Figure 2. The particles of larger size migrate more axially as well as radially than the smaller ones, owing to their higher momentum. The results further indicate that with an increase in swirl the axial and radial displacements generally decrease and increase, respectively, since increased swirl generates a larger centrifugal force. This phenomenon is not always applicable, however, since the smaller particles are sometimes trapped in the reverse circulation flow near the boundary of the jet, and as a result of this they may move inwards towards the center of the jet.

Axial and tangential flight velocities are presented in Figure 3. Since the particles are injected axially (in this example) at a velocity higher than the gas velocity, they decelerate. Moreover, smaller particles encounter much higher drag and decelerate significantly faster. They seem to accelerate somewhat after approximately 1.25 ms as they move slightly towards the center (a zone of higher axial velocity) under the effect of the flow conditions at the boundary of the jet.

Temperature history and conversion are plotted in Figure 4. It is observed that the MoS_2 particles start to melt

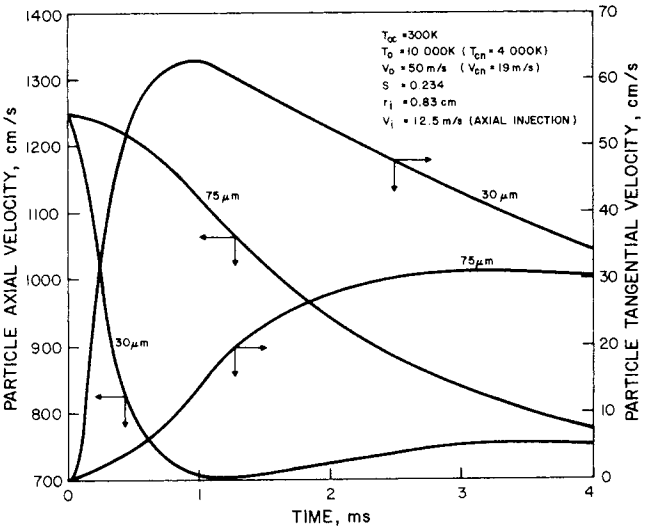

Fig. 3. Axial and tangential components of particle velocity.

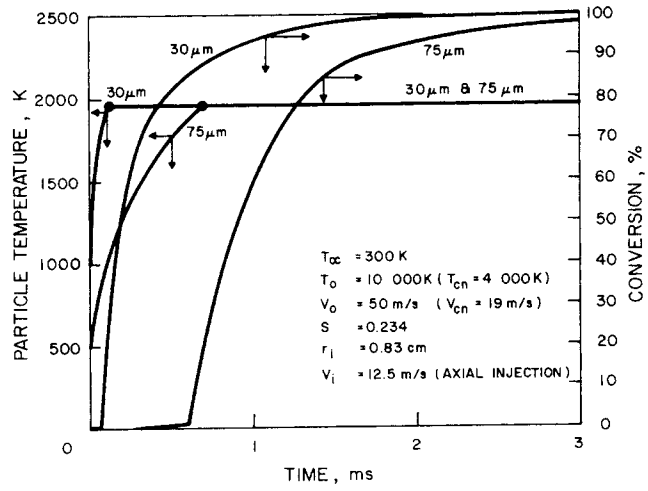

Fig. 4. Particle temperature history and conversion.

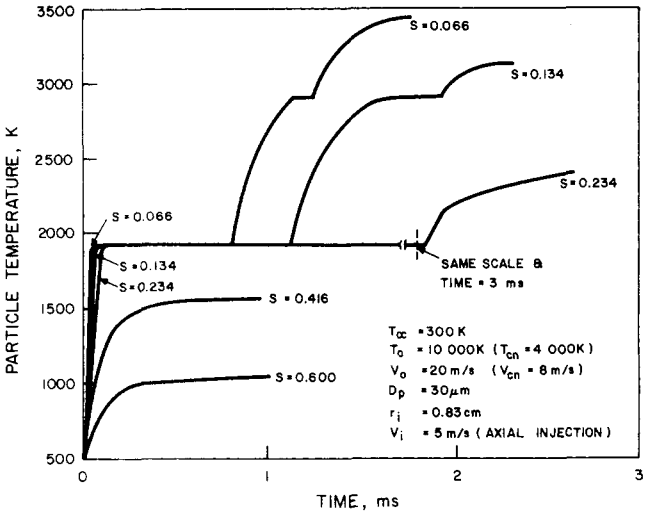

Fig. 5. Effect of swirl on particle temperature history.

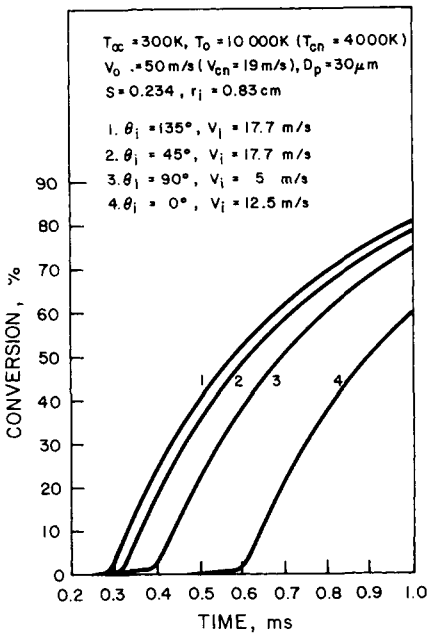

Fig. 6. Effect of angle of injection on conversion.

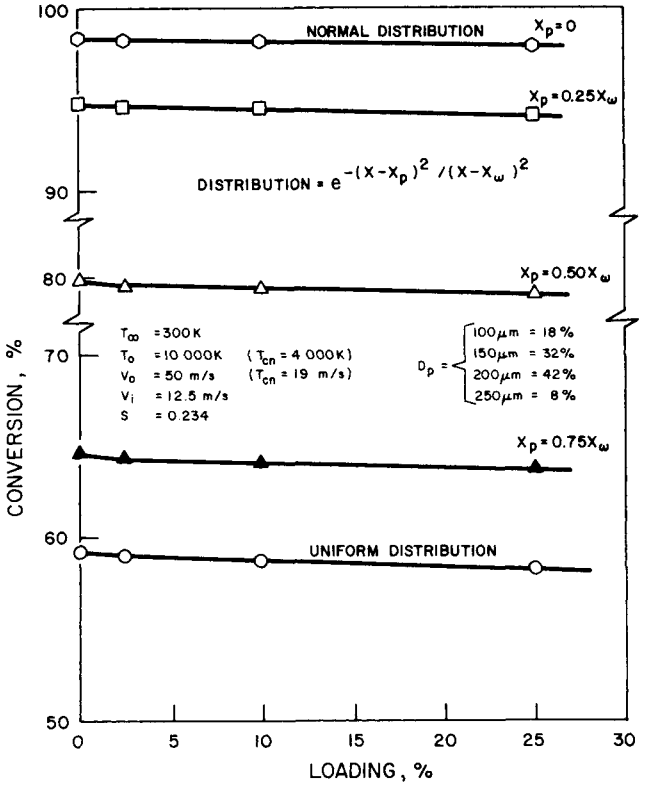

Fig. 7. Effect of particle loading on conversion.

within 0.1 to 0.7 ms after injection. In most cases, the particle residence time is 4 to 5 ms and most of the conversion also takes place in the same period of time for a moderate swirl ($S \leq 0.4$). As shown in Figure 5, swirl has a large influence on the particle thermal history and on the conversion. At high swirls ($S > 0.4$), the 30 μm flakes do not even reach the reaction temperature because of their fast radial migration to a very low temperature zone. At low swirls ($S < 0.234$), however, the Mo metal quickly reaches its boiling point after complete conversion, causing a considerable loss due to vaporization.

The importance of the angle of injection is shown in Figure 6. A forward axial injection velocity up to 12.5 m/s gives the lowest conversion in the present analysis. Maximum conversion is obtained with a back injection at 135 degrees (at 17.7 m/s with both radial and axial components equal to 12.5 m/s). An inward radial injection of 12.5 m/s gives slightly less conversion compared to that with back injection at 17.7 m/s. It is evident that an increase in the radial injection velocity gives rise to a higher conversion, up to a certain limit, after which the particle will penetrate the hottest zone and go to the opposite side of the jet. However, in the case of back injection the particle also moves towards a zone of higher temperature with respect to those in the downstream directions, as in the cases of forward and axial injections.

In the multiparticle case, the effect of larger particle size (100 to 250 μm) due to agglomeration, as well as the effects of loading and concentration and size distributions, have been studied. When loading increases, the gas temperature decays faster and consequently the rate of conversion becomes slower (see Figure 7). However, loading does not affect the overall conversion provided sufficient residence time (10 to 20 ms) is available. It is observed from Figure 7 that a normal concentration distribution of the particles gives the highest conversion, whereas a uniform distribution gives the lowest conversion. This means that the particles should be concentrated near the center of the jet. For the particles of larger size, the conversion largely depends upon the injection location. It is obvious that the closer the injection port is to the center, the higher the conversion will be. A close particle size distribution is also highly desirable for uniformity in product conversion and quality.

In general, nozzle exit velocity, injection velocity, injection location, and jet and ambient temperatures are found to be the important parameters. An increase in conversion is observed with an increased ratio of ambient to the gas temperature at the virtual origin (T_∞/T_0).

It should be noted that all the above results were obtained for an argon plasma. Computations were also carried out for a nitrogen plasma and the results were found to be qualitatively similar. However, nitrogen gave better heat transfer mainly due to its higher thermal conductivity. As a result, in the multiparticle case (100 to 250 μm) with high loading, it is possible to obtain almost complete conversion (99.99%) in a nitrogen plasma. From an industrial point of view, it should be noted, however, that although nitrogen is a cheaper gas than argon power re-

quirements will be higher owing to its higher specific enthalpy.

For example, the generator powers required for an argon and a nitrogen volume-plasma in a 40-cm diameter reactor with a 10-cm diameter coaxial feeding of 100-μm particles for $T_{cn} = 5\,000$ K, $T_\infty = 300$ K, $V_{cn} = 10$ m/s, $V_i = 20$ m/s, $S = 0.234$, $L = 0.25$, $e = 0.1$ and parabolic velocity and temperature profiles are 160 KW and 275 KW, respectively.

ACKNOWLEDGMENT

The authors gratefully acknowledge the financial assistance of the National Research Council of Canada in the form of a Special Grant to the Plasma Technology Group of the Department of Chemical Engineering of McGill University.

NOTATION

a, A = constants, Equations (15) and (14)
b, B = constants, Equations (20) and (14)
C = constant, Equation (14)
C_A = coefficient for added mass
C_D = drag coefficient
C_H = coefficient for Basset history term
C_p = heat capacity
D_{eq} = equivalent particle diameter
D_0 = nozzle diameter
D_0^1 = modified nozzle diameter
D_p = particle diameter
D_p^1 = equivalent particle diameter of a flake, Equation (31)
e = l/D_p, aspect ratio
f_1, f_2 = functional parameters
F = force
g = acceleration due to gravity
G = $V\phi_m/V_{cn}$, velocity ratio
G_z, G_ϕ = axial fluxes of linear and angular momentums, respectively
h = heat transfer coefficient
k = thermal conductivity
K = curl of fluid velocity, Equation (26)
K_1, K_2, K_3 = constants, Equations (11) through (13)
l = length of flake
L = wt of solid/wt of gas, loading ratio
$\dot{m}$ = mass flux
q_r = radiative heat flux
r = radial distance
r_1 = core radius
r_5 = velocity half-radius
r_5^1 = temperature half-radius
R_0 = nozzle radius
R_p = particle radius
S^1 = shape factor
T = temperature
U_r = relative velocity
V = $\sqrt{(V_{fz} - V_{pz})^2 + (V_{fr} - V_{pr})^2 + (V_{f\phi} - V_{p\phi})^2}$, total velocity
V_i = injection velocity
X = radial location for concentration distribution
X_p = location for highest concentration
X_w = radius of feeding zone
z = axial distance

Greek Letters

Δ = increment
$\theta, \theta_0, \theta^1$ = time
θ_i = angle of injection
λ = heat of reaction
μ = viscosity
ν = kinematic viscosity
ξ = r/z, dimensionless distance
ρ = density
ϕ = angular direction

Dimensionless Groups

B^1 = $C_{pv}\Delta T/(\lambda - q_r/\dot{m})$, modified Spalding number
Nu = hD_{eq}/k_f, Nusselt number
Pr = $C_{pf}\mu_f/k_f$, Prandtl number
Pr_t = $(r_5/r_5^1)^2$, turbulent Prandtl number
Re = $D_{eq}V\rho_f/\mu_f$, Reynolds number
S = $G_\phi/(G_z R_0)$, swirl number

Subscripts

0 = virtual origin
av = average
c = center line
cn = center line at nozzle exit plane in axial direction
f = fluid
i = injection
l = liquid
m = maximum tangential
p = particle
r = radial direction
s = solid
v = vapour
z = axial direction
∞ = ambient
ϕ = angular direction
ϕm = maximum angular at nozzle exit plane

LITERATURE CITED

Aoi, T., "The Steady Flow of Viscous Fluid Past a Fixed Spheroid Obstacle at Small Reynolds Numbers," *J. Phys. Soc. Japan*, **10**, 119 (1955).

Beard, K. V., and H. R. Pruppacher, "A Determination of the Terminal Velocity and Drag of Small Waterdrops by Means of a Wind Tunnel," *J. Atm. Sci.*, **26**, 1066 (1969).

Becker, H. A., H. C. Hottel, and G. C. Williams, "Mixing and Flow in Ducted Turbulent Jets," Ninth Intern. Symp. Comb., pp. 7-19, Academic Press, New York (1963).

Boulos, M. I., and W. H. Gauvin, "Powder Processing in a Plasma Jet: A Proposed Model," *Can. J. Chem. Eng.*, **52**, 355 (1974).

Chedaille, J., W. Leuckel, and A. K. Chesters, "Aerodynamic Studies Carried Out on Turbulent Jets by the International Flame Research Foundation," *J. Inst. Fuel*, **39**, 506 (1966).

Chigier, N. A., and J. M. Beér, "Velocity and Static Pressure Distributions in Swirling Air Jets Issuing from Annular and Divergent Nozzles," *Trans. ASME, J. Basic Eng.*, **86**, 788 (1964).

———, and A. Chervinsky, "Experimental and Theoretical Study of Turbulent Swirling Jets Issuing From a Round Orifice," *Israel J. Tech.*, **4**, 44 (1966).

———., "Experimental Investigation of Swirling Vortex Motion in Jets," *Trans. ASME, J. Appl. Mech.*, **34**, 443 (1967).

Domingos, J. J. D., and L. F. C. Roriz, "The Prediction of Trajectories of Evaporating or Buring Droplets," paper presented Fifth Intern. Heat Transfer Conf., Tokyo (1974).

Freeman, M. P., "Chemical Research in Streaming Thermal Plasmas," in *Adv. High Temperature Chem.*, L. Eyring (ed.), Vol. 2, pp. 151-202, Academic Press, New York (1969).

Gal, G., "Self-Preservation in Fully Expanded Turbulent Coflowing Jets," *AIAA J.*, **8**, 814 (1970).

Gauvin, W. H., S. Katta, and F. H. Knelman, "Drop Trajectory Predictions and Their Importance in the Design of Spray Dryers," *Intern. J. Multiphase Flow*, **1**, 793 (1975).

Görtler, H., "Decay of Swirl in an Axially Symmetrical Jet, Far From Orifice," *Revista Math. Hispano Americanas*, **4**, 143 (1954).

Happel, J., and H. Brenner, *Low Reynolds Number Hydrodynamics*, 1st edit., pp. 220-224, Prentice-Hall, Englewood Cliffs, N. J. (1965).
JANAF Thermochemical Tables, Dow Chemical Co., D. R. Stull (ed.), Clearinghouse for Fed. Scientific and Tech. Information, Springfield, Va. (1967).
Kerr, N. M., "Swirl. Part II: Effect on Flame Performance and the Modelling of Swirling Flames," *J. Inst. Fuel.*, **38**, 527 (1965).
———., and D. Fraser, "Swirl, Part I: Effect on Axysymmetrical Turbulent Jets," *J. Inst. Fuel*, 38, 519 (1965).
Lawler, M. T., and P. C. Lu, *Advances in Solid-Liquid Flow in Pipes and its Application*, Iraj Zandi (ed.), pp. 39-57, Pergamon Press, New York (1970).
Lewis, J. A., and W. H. Gauvin, "The Motion of Particles Entrained in a Plasma Jet.," *AIChE J.*, **19**, 982 (1973).
Loitsyanskii, L. G., "The Propagation of a Twisted Jet in an Unbounded Space Filled With the Same Fluid," *Prikkladnaya Mate. Mekhan*, **17**, 3 (1953).
Masliyah, J., and N. Epstein, "Numerical Study of Steady Flow Past Spheroids," *Fluid Mech.*, **44**, 493 (1970).
Maxwell, B. R., "Metallic Particle Residence Criterion for Plasma Spray Applications," *J. Metals*, (3), 53 (1974).
Munz, R. J., "The Decomposition of Molybdenum Disulphide in an Induction Plasma Tailflame," Ph.D. dissertation, McGill Univ., Can. (1974).
O'Connor, T. J., E. H. Comfort, and L. A. Cass, "Turbulent Mixing of an Axisymmetric Jet of Partially Dissociated Nitrogen with Ambient Air," *AIAA J.*, **4**, 2026 (1966).
Pratte, B. D., and J. F. Keffer, "Swirling Turbulent Jet Flows, Part I: The Single Swirling Jet," Rep. No. UTME-TP6901, Univ. Toronto, Can. (1969).
———., "The Swirling Turbulent Jet," *Trans. ASME, J. Basic Eng.*, **92**, 739 (1972).
Ranz, W. E., and W. R. Marshall, "Evaporation From Drops," *Chem. Eng. Progr.*, **48**, 141, 173 (1952).
Ross, L. L., and T. W. Hoffman, "Evaporation of Droplet in a High Temperature Environment," *Proc. Third Intern. Heat Transfer Conf.*, Am. Inst. Chem. Engrs., Chicago, **5**, 50 (1966).
Saffman, P. G., "The Lift on a Small Sphere in a Slow Shear Flow," *J. Fluid Mech.*, **22**, 385 (1965).
Sheer, C., S. Korman, D. J. Angier, and R. P. Cahn, "Arc Vaporization of Refractory Powders," paper presented at 2nd Intern. Symp. Electrochem. Soc., Boston (1973).
Thring, M. W., and M. P. Newby, *Combustion Length of Enclosed Turbulent Jet Flames*, Fourth Intern. Symp. Comb., pp. 789-796, William and Wilkins, Baltimore (1953).
Townsend, A., "The Structure of Shear Flow," 1st. edit., pp. 182-186, Cambridge Univ. Press, England (1956).

Manuscript received December 26, 1974; revision received and accepted April 16, 1975.

Synthesis of Separation Sequences by Ordered Branch Search

An efficient and algorithmic procedure is developed for the synthesis of multicomponent separation sequences. The procedure involves list processing of the possible separation subproblems followed by an ordered branch search to find the optimal sequence with respect to system structure. The technique is conveniently represented by an and/or directed graph. The distribution of sequence costs for a separation problem is considered. When a wide distribution exists, only a minimum of separators need be analyzed to find the optimal sequence. Even when a narrow distribution of sequence costs exists, not all sequences must be developed. The importance of near optimal sequences is examined, and the search procedure is extended to find those sequences whose costs are within a specified factor of the cost of the optimal sequence.

FERNANDO R. RODRIGO B.

and

J. D. SEADER

Department of Chemical Engineering
The University of Utah
Salt Lake City, Utah 84112

SCOPE

Chemical processes frequently involve separation of multicomponent mixtures into multiple products by a sequence of separators, each of which produces generally two, but sometimes more than two, product or intermediate streams. The products may consist of relatively pure species, or they may be multicomponent products that contain two or more major species. In general, the separations are effected by thermal, mechanical, or chemical means. The task of synthesizing the optimal separation sequence often represents a formidable combinatorial problem.

As reviewed by Ichikawa (1972) and Hendry et al. (1973), early research on the synthesis of separation sequences (primarily sequences involving only ordinary distillation) was directed towards the identification of useful heuristics. The application of heuristics permits the design engineer to quickly synthesize reasonable distillation sequences without performing design calculations. More recently, emphasis in synthesis research has shifted to the development of computerized search methods that require design calculations but allow consideration of a variety of separation techniques.

Thompson and King (1972b) used heuristic and algorithmic programming to search for separation sequences. Although their method does not guarantee an optimal

Correspondence concerning this paper should be addressed to J. D. Seader. F. R. Rodrigo B. is now with Universidad Nacional Mayor de San Marcos, Lima, Peru.